Modelling the impact of imperfections in high index-contrast photonic waveguides.

M. Skorobogatiy[a],

[a] École Polytechnique de Montréal, Génie physique,
C.P. 6079, succ. Centre-Ville Montréal, QC, Canada H3C 3A7

ABSTRACT

By formulating Maxwell's equations in perturbation matched curvilinear coordinates, we have derived the rigorous perturbation theory (PT) and coupled mode theory (CMT) expansions that are applicable in the case of generic non-uniform dielectric profile perturbations in high index-contrast waveguides, including photonic band gap fibers, 2D and 3D waveguides. PT is particularly useful in the optimization stage of a component design process where fast evaluation of an optimized property with changing controlling variables is crucial. We demonstrate our method by studying radiation scattering due to common geometric variations in planar 2D photonic crystals waveguides. We conclude the paper by statistical analysis of experimental images of 2D planar PCs to characterize common imperfections in such structures.

Keywords: perturbation theory, coupled mode theory, planar photonic crystals, imperfections

1. INTRODUCTION

Standard perturbation and coupled mode theory formulations are known to fail or exhibit a very slow convergence[1–6] when applied to the analysis of geometrical variations in the structure of high index-contrast waveguides. In a uniform coupled mode theory framework (waveguide profile remains unchanged along the direction of propagation), eigenvalues of the matrix of coupling elements approximate the values of the propagation constants of a uniform waveguide of perturbed cross-section. When large enough number of modes are included coupled mode theory, in principle, should converge to an exact solution for perturbations of any strength. Perturbation theory is numerically more efficient method than coupled mode theory, but it is mostly applicable to the analysis of small perturbations. For stronger perturbations, higher order perturbation corrections must be included converging, in the limit of higher orders, to an exact solution. In a non-uniform (waveguide profile is changing along the direction of propagation) coupled mode and perturbation theories one propagates the modal coefficients along the length of a waveguide using a first order differential equation involving a matrix of coupling elements. Both uniform and non-uniform coupled mode and perturbation theory expansions rely on the knowledge of correct coupling elements.

Conventional approach to the evaluation of the coupling elements proceeds by expansion of the solution for the fields in a perturbed waveguide into the modes of an unperturbed system, then computes a correction to the Hamiltonian of a problem due to the perturbation in question and, finally, computes the required coupling elements. Unfortunately, this approach encounters difficulties when applied to the problem of finding perturbed electromagnetic modes in the waveguides with shifted high index-contrast dielectric boundaries. In particular, for a uniform geometric perturbation of a fiber profile with abrupt high index-contrast dielectric interfaces, expansion of the perturbed modes into an increasing number of the modes of an unperturbed system does not converge to a correct solution when standard form of the coupling elements[7,8] is used. Mathematical reasons of such a failure are still not completely understood but probably lie either in the *incompleteness* of the basis of eigenmodes of an unperturbed waveguide in the domain of the eigenmodes of a perturbed waveguide or in the fact that the standard mode orthogonality conditions (4.1) do not constitute strict norms. We would like to point out that standard coupled mode theory can still be used even in the problem of finding the modes of a high index-contrast waveguide with sharp dielectric interfaces. One can calculate such modes by using as an expansion basis eigen modes of some reference waveguide with "smooth" dielectric profile (empty metallic waveguide, for example). However, the convergence of such a method with respect to the number of basis modes is slow (linear). Perturbation formulation within this approach is also problematic, and even for small geometric variations of waveguide profile matrix of coupling element has to be recomputed anew. Other methods developed to deal with shifting metallic boundaries and dielectric interfaces originate primarily from the works on metallic waveguides and microwave circuits.[9–14] Dealing with non-uniform waveguides, these formulations usually employ an expansion

Send e-mail to: maksim.skorobogatiy@polymtl.ca

Photonic Crystal Materials and Devices III, edited by Ali Adibi, Shawn-Yu Lin, Axel Scherer,
Proc. of SPIE Vol. 5733 (SPIE, Bellingham, WA, 2005) · 0277-786X/05/$15 · doi: 10.1117/12.589730

basis of the "instantaneous modes". Such modes have to be recalculated at each different waveguide cross-section leading to potentially computationally demanding propagation schemes. When high index waveguide exhibit only cylindrical features multipole method and its derivatives could be used to analyze the eigen modes and scattering in such waveguides,[15–19] however these methods do not allow perturbative formulation. Finally, time domain codes[20] are usually difficult to apply to analysis of small variation and imperfections as one has to use meshes fine enough to resolve the imperfections, and model large propagation distances over which the effects of small variations become discernable. Similarly, frequency domain and mode matching methods[21–25] require large supercells and fine resolution to capture the impact of small perturbations.

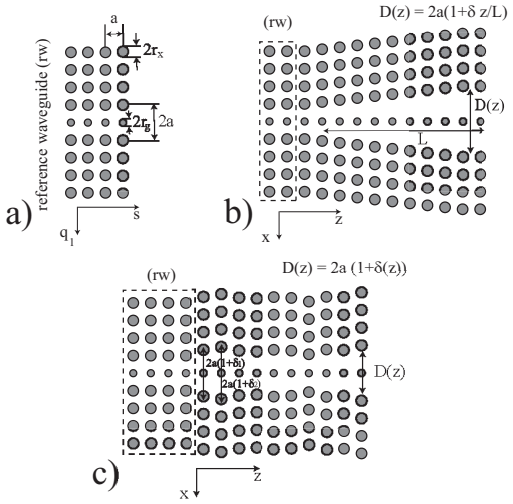

Figure 1. a) Dielectric profile of a reference 2D photonic crystal waveguide as formed in a square array of dielectric poles in the air by a linear sequence of somewhat smaller dielectric poles. b) Linear taper in a photonic crystal with "unzipping" photonic mirror c) Stochastic variations in a waveguide core size along the direction of propagation

In this paper we introduce a method of evaluating the coupling elements which is valid for any smooth geometrical waveguide profile variations and high index contrast using the eigen modes of an unperturbed waveguide (to which we refer as a reference waveguide) as an expansion basis. This paper presents generalization of an earlier method developed to analyze imperfections in high index-contrast fibers.[1,30] Main idea of our method is to introduce a coordinate transformation that maps a dielectric profile of a reference waveguide (whose eigen modes are assumed to be known) onto a dielectric profile of a perturbed waveguide. Such mappings can be either defined analytically or computed numerically. Transforming Maxwell's equations into a curvilinear system where dielectric profile is unperturbed we can use the eigen modes of a reference waveguide as an expansion basis. These modes will be now coupled due to the curvature of the space, which is in turn, proportional to the strength of the perturbation in question. Another interpretation of the same methodology is to use the eigen modes of a reference waveguide and to stretch them using a coordinate mapping in such a way as to make the discontinuities in their fields to coincide with position of the perturbed dielectric interfaces, and to finally use such stretched, perturbation fitted modes as an expansion basis. In further discussions we formulate geometrical waveguide profile variations in terms of a smooth mapping of an unperturbed dielectric profile onto a perturbed one. Given a perturbed dielectric profile $\epsilon(x,y,z)$ in a Euclidian system of coordinates (x,y,z) (where z is a general direction of propagation) we define a mapping $(x(q^1,q^2,s), y(q^1,q^2,s), z(q^1,q^2,s))$ such that $\epsilon(q^1,q^2,s)$ corresponds to a dielectric profile of a reference waveguide in a curvilinear coordinate system associated with (q^1,q^2,s) (where s is a direction of propagation). We then perform a coordinate transformation from a Euclidian coordinate system (x,y,z) into a corresponding curvilinear coordinate system (q^1,q^2,s) by rewriting Maxwell's equations in such a curvilinear coordinate system. Finally, as the dielectric profile in a coordinate system (q^1,q^2,s) is that of a reference waveguide, we can use the basis set of its eigen modes in (q^1,q^2,s) coordinates to calculate coupling matrix elements due to the geometrical variations of a waveguide profile.

Our paper is organized as following. We first describe some typical geometrical variations of 2D waveguide profiles. Next, we discuss properties of generic curvilinear coordinate transformations and formulate Maxwell's equations in a curvilinear coordinate system. We apply this formulation to develop the coupled mode and perturbation theories using eigen states of an unperturbed waveguide as an expansion basis. We then present analysis of several typical variations in 2D waveguides. We conclude with statistical analysis of experimental imperfections from the images of 2D planar photonic crystals.

2. GEOMETRICAL VARIATIONS OF WAVEGUIDE PROFILES

We start by considering several common geometrical variations of waveguide profiles that can be either deliberately designed or arise during manufacturing as im-

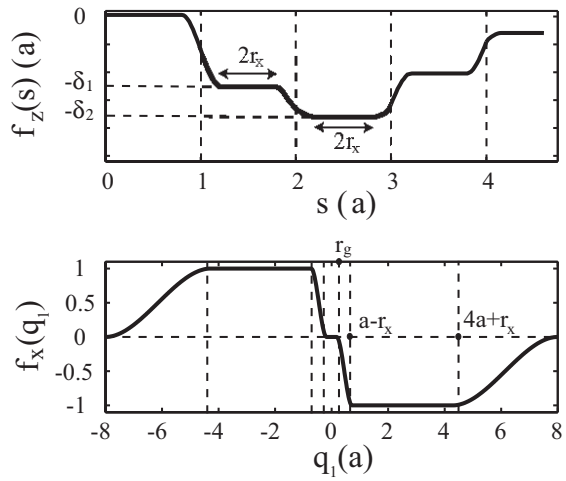

Figure 2. Auxiliary functions for the coordinate mapping of a reference 2D photonic crystal waveguide (Fig. 1a)) onto a waveguide of a changing core size (Fig. 1c))

perfections. Let (x, y, z) correspond to Euclidian coordinate system. In Fig. 1a) an ideal 2D photonic crystal waveguide is presented. In what follows the operation frequency and all the waveguide dimensions are chosen for a reference waveguide to be singlemoded, with forward and backward propagating fundamental modes confined by the bandgap of the reflector. In Fig. 1b) the photonic crystal taper with "unzipping" mirror is presented. When the core size is increased sufficiently, the fundamental mode becomes purely guided by the high index of the remaining corrugated waveguide. In Fig. 1c) a waveguide with arbitrarily changing core size along the direction of propagation is presented. When such variations are small and random one can consider them to be a model of roughness.

We now define a dielectric profile mapping of a reference photonic crystal waveguide Fig. 1a) onto a waveguide with a changing core size Fig. 1c) by using the mapping $x = q_1 + f_x(q_1)f_z(s), y = q_2, z = s$, where auxiliary functions $f_x(q_1)$ and $f_z(s)$ are chosen to be as on Fig. 2. As seen from this figure, in each of the unit cells along the waveguide length the functions $f_x(q_1)$ and $f_z(s)$ are defined in such a way as to translate the reflector rods along the x direction by an appropriate value of the core size change, while leaving the smaller rods of a defect waveguide intact. These auxiliary functions and their first derivatives have to be continuous everywhere. Although only the variations in the waveguide core size are considered in this paper the CMT derived in this article is general. For other variations corresponding coordinate mappings can be computed analytically or numerically from the original and final positions of the dielectric interfaces.

3. CURVILINEAR COORDINATE SYSTEMS

Following,[26,27] we first introduce general properties of the curvilinear coordinate transformations. Let (x^1, x^2, x^3) be the coordinates in a Euclidian coordinate system. We introduce a smooth mapping (requiring continuity of the functions and all their partial derivatives in the computation domain) into a new coordinate system with coordinates (q^1, q^2, q^3) as $(x^1(q^1, q^2, q^3), x^2(q^1, q^2, q^3), x^3(q^1, q^2, q^3))$. A new coordinate system can be characterized by its covariant basis vectors $\vec{a}_i$ defined in the original Euclidian system as $\vec{a}_i = (\frac{\partial x^1}{\partial q^i}, \frac{\partial x^2}{\partial q^i}, \frac{\partial x^3}{\partial q^i})$. Now, define reciprocal (contravariant) vector $\vec{a}^i$ as $\vec{a}^i = \frac{1}{\sqrt{g}}\vec{a}_j \times \vec{a}_k, \quad (k, j) \neq i$, where metric g_{ij} is defined as $g_{ij} = \frac{\partial x^k}{\partial q^i}\frac{\partial x^k}{\partial q^j}$, and $g = det(g_{ij})$. Vectors $\vec{a}_i$ and their reciprocal $\vec{a}^i$ satisfy the following orthogonality conditions $\vec{a}^i \cdot \vec{a}_j = \delta_{i,j}$, $\vec{a}_i \cdot \vec{a}_j = g_{ij}$, $\vec{a}^i \cdot \vec{a}^j = g^{ij}$, where g^{ij} is an inverse of the metric g_{ij}. In general, a vector may be represented by its covariant components $\vec{E} = e_i\vec{a}^i$ or by its contravariant components $\vec{E} = e^i\vec{a}_i$. These components might have unusual dimensions because the underlying vectors $\vec{a}_i$ and $\vec{a}^i$ are not properly normalized in a Euclidian coordinate system. Components having the usual dimensions are defined by $E_i = \frac{e_i}{\sqrt{g^{ii}}}$, $E^i = \frac{e^i}{\sqrt{g_{ii}}}$ and $\vec{E} = e_i\vec{a}^i = E_i\vec{i}^i, \vec{E} = e^i\vec{a}_i = E^i\vec{i}_i$, where $\vec{i}_i, \vec{i}^i$ are unitary vectors. Normalized covariant and contravariant components are connected by $E_i = G_{ij}E^j$, $E^i = G^{ij}E_j$ where $G_{ij} = \sqrt{\frac{g^{ii}}{g_{jj}}}g_{ij}$, $G^{ij} = \sqrt{\frac{g_{ii}}{g^{jj}}}g^{ij}$. For orthogonal coordinate systems the metric matrixes are diagonal and for the regular orthogonal and polar coordinate systems they are $g^{0xx} = 1; g^{0yy} = 1; g^{0zz} = 1; g^0 = 1$, and $g^{0\rho\rho} = 1; g^{0\theta\theta} = \frac{1}{\rho^2}; g^{0zz} = 1; g^0 = \rho^2$ correspondingly.

4. COUPLED MODE THEORY FOR MAXWELL'S EQUATIONS IN CURVILINEAR COORDINATES

In the following, we summarize coupled mode theory for Maxwell's equations in curvilinear coordinates to treat radiation propagation in generic non-uniform waveguides. Hamiltonian formulation of Maxwell's equations in regular Euclidian coordinates is detailed in,[2,3,13] while Hamiltonian formulation and coupled mode theory in curvilinear perturbation matched coordinates for the case of uniform and non-uniform fibers of arbitrary cross-sections is detailed in.[3,4,30,31]

The form of Maxwell's equations in curvilinear coordinates can be found in a variety of references.[26–29] Assuming the standard time dependence of the electro-magnetic fields $\mathbf{F}(q_1,q_2,q_3,t) = \mathbf{F}(q_1,q_2,q_3)\exp(-i\omega t)$, ($\mathbf{F} = (\frac{E_{q_1}}{\sqrt{g^{11}}};\frac{E_{q_2}}{\sqrt{g^{22}}};\frac{E_{q_3}}{\sqrt{g^{33}}};\frac{H_{q_1}}{\sqrt{g^{11}}};\frac{H_{q_2}}{\sqrt{g^{22}}};\frac{H_{q_3}}{\sqrt{g^{33}}})$ denotes a 6 component column vector of the electro-magnetic fields) these expressions are compactly presented in terms of the normalized covariant components of the fields, and in the absence of free electric currents they are:

$$\begin{aligned} -i\omega\epsilon(q^1,q^2,q^3)D^{ij}\frac{E_j}{\sqrt{g^{jj}}} &= e^{ijk}\frac{\partial\frac{H_k}{\sqrt{g^{kk}}}}{\partial q^j} \\ i\omega\mu(q^1,q^2,q^3)D^{ij}\frac{H_j}{\sqrt{g^{jj}}} &= e^{ijk}\frac{\partial\frac{E_k}{\sqrt{g^{kk}}}}{\partial q^j}, \end{aligned} \quad (1)$$

where $D^{ij} = \sqrt{g}g^{ij}$, and e^{ijk} is a Levi-Civita symbol.

4.1. Modal orthogonality relations and normalization

In the following we assume that reference waveguide is either uniform (planar waveguide, fiber) or strictly periodic (photonic crystal waveguide, fiber grating) along the direction of propagation $q^3 = s$. This implies that both ϵ_0 and μ_0 (marking parameters related to reference waveguide with a subscript zero) either do not depend on s, or they are periodic functions of s. We assume that eigen modes and eigen values of a reference waveguide are found in a coordinate system with a diagonal (non necessarily unitary) space metric corresponding to orthogonal coordinate system. Several orthogonality relations between the eigen modes of a reference waveguide are possible.

A norm operator $\hat{B}$ and its matrix representation[13] can be introduced as:

$$\hat{B} = \begin{pmatrix} 0 & 0 & 0 & 0 & 1 & 0 \\ 0 & 0 & 0 & -1 & 0 & 0 \\ 0 & 0 & 0 & 0 & 0 & 0 \\ 0 & -1 & 0 & 0 & 0 & 0 \\ 1 & 0 & 0 & 0 & 0 & 0 \\ 0 & 0 & 0 & 0 & 0 & 0 \end{pmatrix}, \quad (2)$$

relating the transverse components of the eigen fields. Depending upon the symmetry of a reference waveguide several orthogonality relations are possible:

If reference waveguide profile is uniform along s, then the eigen fields have an additional symmetry $\mathbf{F}(q^1,q^2,s) = \mathbf{F}_\beta(q^1,q^2)\exp(i\beta s)$.
1) If ϵ_0 and μ_0 are strictly real we introduce Dirac notation as $|\beta\rangle = \mathbf{F}_\beta(q^1,q^2)$ and $\langle\beta| = \mathbf{F}^+_\beta(q^1,q^2)$, and a product operator $\langle\beta_i|\hat{O}|\beta_j\rangle = \int_{cros} dq^1dq^2\mathbf{F}^+_{\beta_i}(q^1,q^2)O\mathbf{F}_{\beta_j}(q^1,q^2)$, where O is a $6X6$ operator matrix, and integration is performed over the waveguide crossection. Then, for any two eigen modes labelled by their propagation constants β_i, β_j the eigen modes can be normalized as $\langle\beta_i|\hat{B}|\beta_j\rangle = \delta_{\beta_1^*,\beta_j}\eta_{\beta_j}$, and $|\eta_{\beta_j}| = 1$.
2) If ϵ_0 or μ_0 has a complex part, we introduce Dirac notation as $|\beta\rangle = \mathbf{F}_\beta(q^1,q^2)$ and $\langle\beta| = \mathbf{F}_\beta(q^1,q^2)$, (no complex conjugation) and a product operator $\langle\beta_i|\hat{O}|\beta_j\rangle = \int_{cros} dq^1dq^2\mathbf{F}^T_{\beta_i}(q^1,q^2)O\mathbf{F}_{\beta_j}(q^1,q^2)$, where integration is performed over the waveguide crossection. Then for any two eigen modes labelled by their propagation constants β_i, β_j the eigen modes can be normalized as $\langle\beta_i|\hat{B}|\beta_j\rangle = \delta_{\beta_i,\beta_j}\eta_{\beta_j}$, and $|\eta_{\beta_j}| = 1$.

If unperturbed waveguide profile is periodic along s with period Λ then according to the Bloch-Floquet theorem the eigen fields still retain a symmetry $\mathbf{F}(q^1,q^2,s) = \mathbf{F}_\beta(q^1,q^2,s)\exp(i\beta s)$, where $\mathbf{F}_\beta(q^1,q^2,s) = \mathbf{F}_\beta(q^1,q^2,s+\Lambda)$. If ϵ_0 and μ_0 are strictly real we introduce Dirac notation as $|\beta\rangle = \mathbf{F}_\beta(q^1,q^2,s)$ and $\langle\beta| = \mathbf{F}^+_\beta(q^1,q^2,s)$, as well as a product operator $\langle\beta_i|\hat{O}|\beta_j\rangle = \int_{cell} dq^1dq^2ds\mathbf{F}^+_{\beta_i}(q^1,q^2,s)O\mathbf{F}_{\beta_j}(q^1,q^2,s)$, where O is a $6X6$ operator matrix and integration is performed over the whole unit cell of a periodic waveguide. Then for any two eigen modes labelled by their propagation constants β_i, β_j the eigen modes can be normalized as $\langle\beta_i|\hat{B}|\beta_j\rangle = \delta_{\beta_1^*,\beta_j}\eta_{\beta_j}$, and $|\eta_{\beta_j}| = 1$. Moreover, a corollary of Bloch-Floquet theorem states that the eigen modes at β and $\beta + 2\pi l/\Lambda$ are equivalent for any integer l, and thus $|\beta + 2\pi l/\Lambda\rangle = \exp(-2\pi i l/\Lambda z)|\beta\rangle$. This implies that it suffices to choose all the eigen values β in the first Brillouin zone $Re(\beta) \in (-\pi/\Lambda, \pi/\Lambda]$, and for such modes definition of the norm can be furthermore relaxed to be $\langle\beta_i|\hat{B}|\beta_j\rangle = \int_{cell} dq^1dq^2ds\mathbf{F}^+_{\beta_i}(q^1,q^2,s)B\mathbf{F}_{\beta_j}(q^1,q^2,s) = \Lambda\int_{cros} dq^1dq^2\mathbf{F}^+_{\beta_i}(q^1,q^2,s)B\mathbf{F}_{\beta_j}(q^1,q^2,s)$, where the integral over a reference waveguide crossection is invariant for any crossection (any s) in the first Brilloun zone. Thus, the definition of the norm in the case of real ϵ_0 and μ_0 for periodic and uniform waveguides can be chosen to be the same.

4.2. Expansion basis and coupled mode theory

We now construct an expansion basis to treat radiation propagation in a perturbed waveguide using the eigen fields of a reference waveguide in the perturbation matched curvilinear coordinate system. Equivalently, in the Euclidian coordinate system associated

with a perturbed waveguide we construct an expansion basis from the eigen fields of an unperturbed waveguide by spatially stretching them in such a way as to match the regions of discontinuity in their field components with the position of the perturbed dielectric interfaces. Finally, we find expansion coefficients by satisfying Maxwell's equations. In the following, we first define an expansion basis and then demonstrate how perturbation theory and a coupled mode theory can be formulated in such a basis.

Let (x, y, z) to define a Euclidian coordinate system associated with a perturbed waveguide, and (q^1, q^2, s) be a coordinate system corresponding to an unperturbed waveguide, where s is a direction of propagation, with corresponding smooth coordinate transformation relating the two coordinate systems being $(x(q^1, q^2, s), y(q^1, q^2, s), z(q^1, q^2, s))$. Maxwell's equations in curvilinear coordinates (1), while seemingly complicated, involve an unperturbed dielectric profile $\epsilon(q^1, q^2, s)$. We look for a solution of Maxwell's equations (1) in terms of the basis fields which in (q^1, q^2, s) coordinate system are the eigen fields of a reference waveguide entering with corresponding varying along the direction of propagation coefficients $C^{\beta}(s)$. Thus, in the covariant coordinates for both uniform and periodic waveguides we look for a solution in a form:

$$\begin{pmatrix} \frac{E_{q^1}(q^1,q^2,s)}{\sqrt{g^{q^1q^1}}} \\ \frac{E_{q^2}(q^1,q^2,s)}{\sqrt{g^{q^2q^2}}} \\ \frac{H_{q^1}(q^1,q^2,s)}{\sqrt{g^{q^1q^1}}} \\ \frac{H_{q^2}(q^1,q^2,s)}{\sqrt{g^{q^2q^2}}} \end{pmatrix} = \sum_{\beta_j} C^{\beta_j}(s) \begin{pmatrix} \frac{E^0_{q^1}(q^1,q^2,s)}{\sqrt{g^{0q^1q^1}}} \\ \frac{E^0_{q^2}(q^1,q^2,s)}{\sqrt{g^{0q^2q^2}}} \\ \frac{H^0_{q^1}(q^1,q^2,s)}{\sqrt{g^{0q^1q^1}}} \\ \frac{H^0_{q^2}(q^1,q^2,s)}{\sqrt{g^{0q^2q^2}}} \end{pmatrix}_{\beta_j} . \tag{3}$$

Note, that for a uniform reference waveguide, the expansion fields are functions of (q^1, q^2) only, and for both uniform and periodic reference waveguides basis fields are stripped of the phase factor $\exp(i\beta z)$. Substituting expansion (3) into (1), expressing s components of the fields through the transverse components, using the orthogonality relations of section **4.1** and manipulating the resultant expressions we arrive to the following equations:

$$B\frac{\partial \vec{C}(s)}{\partial s} = i(B\mathcal{B}_0 + \Delta M(s))\vec{C}(s), \tag{4}$$

where $B_{\beta_i,\beta_j} = \langle \beta_i | \hat{B} | \beta_j \rangle$ is a constant normalization matrix, $\mathcal{B}_0$ is a diagonal matrix of eigenvalues of an unperturbed reference waveguide, and $\Delta M(s)$ is a matrix of coupling elements given in.[31]

Presented coupled mode theory describes completely radiation scattering in arbitrary index-contrast waveguides with shifting dielectric boundaries and changing dielectric profile. Moreover, (4) allows perturbative expansion. As metric of a slightly perturbed coordinate system is only slightly different from the metric of an unperturbed coordinate system that will naturally introduce a small parameter for small geometrical perturbations of waveguide profiles. For application of this theory to analysis of variations in high index-contrast fibers see.[3, 4, 30, 31]

5. VARIATIONS IN 2D PHOTONIC CRYSTAL WAVEGUIDES

In further examples we study propagation of TE polarized radiation (electric field is directed out of the xz plane) in a line defect waveguide made of a periodic sequence of high index cylinders of radii $r_g = 0.2a$ embedded in a square lattice of $r_x = 0.3a$ dielectric rods of the reflector.[13] Parameter a defines periodicity of a photonic crystal waveguide in the direction of propagation. All the dielectric rods have index $n = 3.37$. Perfectly conducting boundary conditions were imposed in the x direction $\pm 8a$ from the waveguide center line. The frequency $\omega = 0.25 \times 2\pi c/a$ is chosen so that the waveguide formed solely by a sequence of the dielectric rods of radii $r_g = 0.2a$ is guiding and is singlemoded, while a reference photonic crystal waveguide is also singlemoded guiding in the band gap of the reflector. We use assymptotically exact CAMFR code to compute an expansion basis constructed of the guided and evanescent eigen modes of an unperturbed photonic crystal waveguide defined by the first unit cell in the Fig. 1a). Total of 4 guided modes with real $\beta' s$ (where backward and forward modes with the same absolute values of their propagation constants are counted ones) and up to 58 evanescent modes with complex propagation constants were used in the expansion basis to study convergence of the CMT. Advantage of our coupled mode theory is the use at all points along the propagation direction of a single expansion basis precalculated in advance. This can be of great advantage for computationally demanding simulations of long structures.

5.1. Eigenmodes of a perturbed uniform waveguide

We first study convergence of a CMT when perturbed waveguide remains uniform along the direction of propagation (Fig. 3a)). For such variations, a perturbed waveguide still exhibits eigen modes labelled by a new set of propagation constants. Presented in Fig. 3b) is

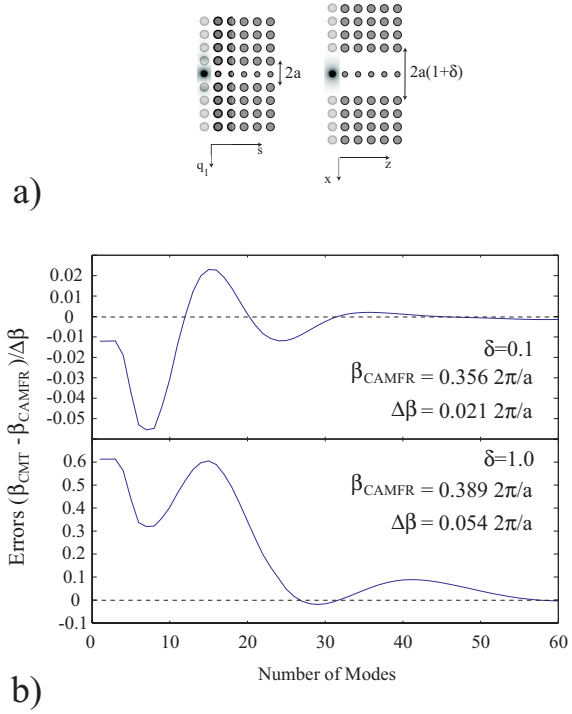

Figure 3. (a) Schematics of a reference waveguide (left) and a perturbed uniform waveguide (right) of a larger core. Electric energy distributions in the fundamental modes are presented in the corresponding first unit cells. (b) Convergence of the fundamental mode propagation constant for a weakly $\delta = 0.1$ and a strongly $\delta = 1.0$ perturbed reference waveguide in a CMT framework.

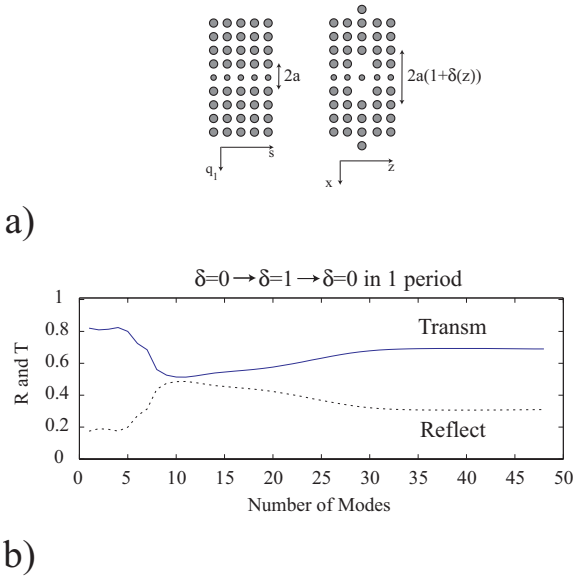

Figure 4. (a) Schematics of a reference waveguide (left) and a single cell defect in a reference waveguide (right). (b) Convergence of the transmitted and reflected powers into the forward and backward propagating fundamental modes as calculated by CMT and $\delta = 1.0$ perturbation.

convergence of a fundamental mode propagation constant for a weakly $\delta = 0.1$ and a strongly $\delta = 1.0$ perturbed reference waveguide in a CMT framework. For $\delta = 0.1$ (top plot), inclusion of a single forward propagating fundamental mode results in errors of only several percents, suggesting validity of a perturbation theory regime for a variation of this magnitude. For $\delta = 1.0$ (bottom plot), variation is large and more than 30 modes are needed to reduce the errors to several percents. In both cases propagation constants calculated by CMT are compared to the propagation constants calculated by asymptotically exact CAMFR code.

5.2. Scattering from abrupt variations in a waveguide core

We next study convergence of the transmitted and reflected powers from an abrupt variation in a waveguide core size. In Fig. 4a) a single cell defect of strength $\delta = 1.0$ is presented. Scattered powers into the forward and backward propagating fundamental modes as calculated by CMT are shown in Fig. 4b). For a strong variation of $\delta = 1.0$, 30 modes are needed for convergence, while convergence is faster than linear when additional modes are added. As in the case of the uniform variations, for small perturbations $\delta < 0.1$ scattering coefficients can be calculated accurately with only a few modes using perturbation theory.

5.3. Scattering from tapers

In Fig. 5a) schematic of a taper between a line defect waveguide in a square lattice of dielectric rods in air and a waveguide formed by a 1D sequence of dielectric rods is presented. To the left and to the right of the taper the photonic crystal is that of a reference waveguide. Many nuances of transmission of a fundamental mode through such a taper for TE polarization have been previously studied in the instantaneous mode framework.[13] We believe that method of instantaneous modes can be more efficient when larger variations (non-adiabatic tapers) are considered, and therefore convergence with a fixed basis is slow. However, for smaller variations (adiabatic tapers) convergence with a fixed basis is efficient, while it becomes costly to re-compute instantaneous expansion basis at different crossections, thus rendering a method employing fixed basis to be more efficient than a method employing instantaneous modes (for detailed

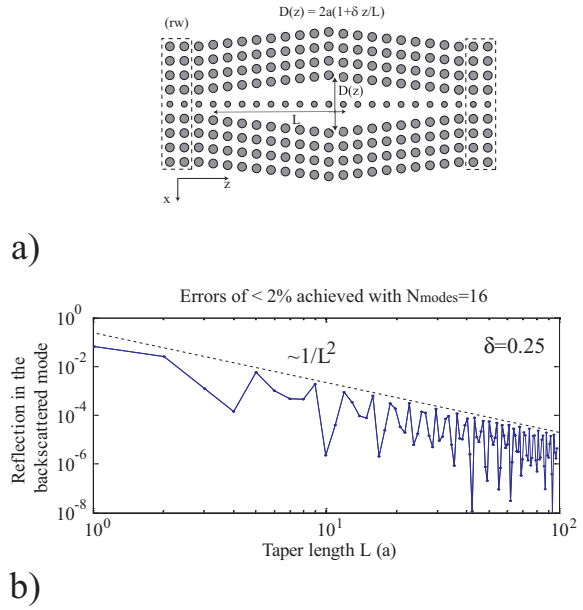

Figure 5. (a) Taper of an "unzipping" reflector around an index guiding waveguide. To the left and to the right of the taper the photonic crystal waveguide is infinite and is described by the first unit cell of the schematic. (b) Reflected power from the taper at $\omega = 0.25 \times 2\pi c/a$ as a function of taper length L. Observe a $1/L^2$ decrease of the reflected power with taper length.

discussion see[9]).

Here we investigate the magnitude of the back scattering into the backward propagating fundamental mode as a function of the taper length. In Fig. 5b) we plot the reflected power from the "unzipping" taper of strength $\delta = 0.25$ at $\omega = 0.25 \times 2\pi c/a$ as a function of the taper length L. Expected $1/L^2$ decrease of the reflected power for the large taper lengths $20 < L < 100$ is clearly observed. It was found that 16 expansion modes were enough to reduce the error in the scattering coefficients below 2%.

5.4. Scattering from random variations in a waveguide core size

We now calculate the strength of back scattering from small stochastic variations in a waveguide core size. Computational domain is defined by taking a reference waveguide and changing the waveguide core size (shifting the lower and upper reflector parts) in each unit cell i by $2a\delta_i$, where $2a$ is a core size of a reference waveguide (Fig. 6a)). Random variable δ_i is considered to be distributed according to the gaussian distribution with variance δ. For each $\delta = 0.0025, 0.005, 0.01, 0.02$ and $\omega = 0.25 \times 2\pi c/a$, back reflected power from a

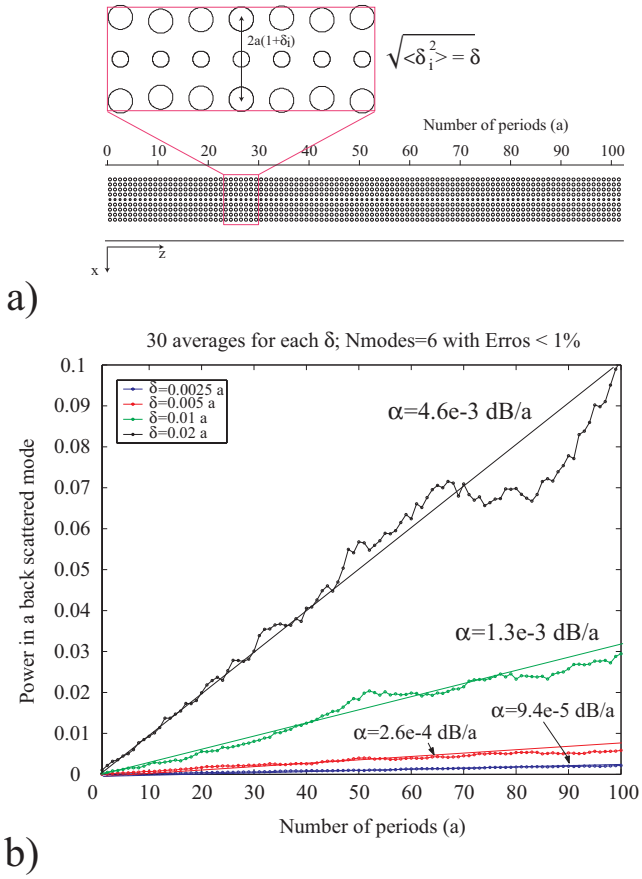

Figure 6. (a) Schematic of a computational domain to study back scattering losses due to waveguide core size variations. Variations in the core size are assumed to be uncorrelated from one unit cell to another, and distributed according to the gaussian distribution with variance δ. (b) For each δ, back reflected power from a waveguide with "roughness" is presented as a function of propagation distance L. Each δ curve represents an average over 30 realizations of "roughness".

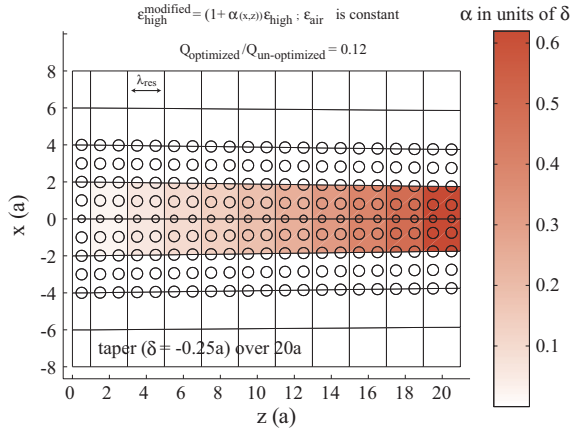

Figure 7. Designing dielectric profile to negate the effects of variations in a waveguide geometry. Presented is an undesired taper of strength $\delta = -0.25$ over the length of 20 unit cells. Square mesh corresponds to the non-overlapping regions where dielectric is modified, thus modelling finite resolution and positioning accuracy of the index changing tool. Values of dielectric constant in various square regions were chosen to make the propagation constant of a perturbed waveguide to match closely the propagation constant of an unperturbed reference waveguide along the whole length of a taper. Only the material of high refractive index is modified $\epsilon_{high}^{modified} = (1 + \alpha(x, z))\epsilon_{high}$. Required change in the dielectric constant $\alpha(x, z)$ is presented in shades. In general, we observe that $\alpha \sim \delta$, consistent with predictions of perturbation theory.

waveguide with stochastic core size variations is presented as a function of propagation distance L. Each δ curve represents an average over 30 realizations of stochastic variations (Fig. 6b)). First, we observe that power in the back scattered fundamental mode scales linearly with the length of propagation L, defining average scattering losses of $9.4 \cdot 10^{-5} dB/a$, $2.6 \cdot 10^{-4} dB/a$, $1.3 \cdot 10^{-3} dB/a$ and $4.6 \cdot 10^{-3} dB/a$ for the corresponding δ's. One also observes δ^2 scaling of losses with perturbation strength. It was found that 6 expansion modes were enough to reduce the errors in the scattering coefficients below 1% for all δ's.

5.5. Compensation of geometrical variations by changing dielectric profile

Finally, we demonstrate how PT expansions can be useful to design dielectric profiles that compensate for the undesired weak variations in a waveguide geometry. One way of changing the dielectric constant of an underlying material could be via an interaction with femtosecond laser radiation. Material interaction with femtosecond radiation is currently actively investigated for writing bulk and planar waveguides in various materials. With such a process index change is proportional to the exposure time to the radiation, while spatial resolution λ_{res} is determined by the laser spot size in focus. Thus, given the spatial resolution ("spot size") of the focused laser beam and positioning resolution of a setup we investigate at what spatial points and with what intensities laser beam has to be applied to reduce the effects of undesired variations.

Particularly, in the case of a weak slow variation (taper, for example), local propagation constant of a fundamental mode $\beta(z)$ at a point z along the waveguide can be approximated by the first order perturbation correction $\beta(z) = \beta_0 + \langle\beta_0|\Delta M_{\beta_0,\beta_0}(z)|\beta_0\rangle \,/\, \langle\beta_0|\hat{B}|\beta_0\rangle$, where β_0 corresponds to the fundamental mode of a reference waveguide, while $\Delta M_{\beta_0,\beta_0}(z)$ and $\hat{B}$ are defined in section **4**. As matrix of coupling elements $M_{\beta_0,\beta_0}(z)$ depends simultaneously on the geometry of variation and underlying dielectric profile, by modifying such a dielectric profile one can, in principle, compensate for the effects of undesired variations in waveguide geometry. To construct optimization problem we can define an objective function as follows:

$$Q = \int_0^L dz|\beta(z) - \beta_0|^2 = \int_0^L dz|\frac{\langle\beta_0|\Delta M_{\beta_0,\beta_0}(z,\epsilon)|\beta_0\rangle}{\langle\beta_0|\hat{B}|\beta_0\rangle}|^2. \tag{5}$$

By minimizing the objective function Q via changing the dielectric profile we force the local propagation constant to be that of an unperturbed reference waveguide, thus negating the effect of an undesired taper. We introduce possible changes in the dielectric profile as $\epsilon = \epsilon_0 + \sum_i c_i \phi(x - x_i, z - z_i)$, where ϵ_0 corresponds to the dielectric profile of a reference waveguide, while spot function $\phi(x - x_i, z - z_i)$ is a localized function defining intensity distribution of a laser spot focused at a point (x_i, z_i). For a set of the focusing points (x_i, z_i) defined by the positioning resolution of the device, unknown coefficients c_i are then chosen to minimize the value of the objective function Q. In general, such formulation leads to a nonlinear optimization problem that can be approached by a variety of well established numerical methods. Finally, modified dielectric profile is reconstructed using optimal c_i's, and success of optimization is judged by the ratio of $Q_{optimal}/Q_{un-optimized}$.

In Fig. 7 we present the results of optimization of the dielectric profile to negate the effects of an undesired taper of strength $\delta = -0.25$ over the length of $L = 20$ unit cells. Waveguide on the left of the taper is assumed to be infinite and described by the leftmost unit cell of the taper. Spot function $\phi(x - x_i, z - z_i)$ is chosen to be

unity defined on a square of size $\lambda_{res} = 2a$. It is also assumed that only the high index dielectric can be modified $\epsilon_{high}^{modified} = (1+\alpha(x,z))\epsilon_{high}$. Focus points (x_i, z_i) were chosen to create a square mesh of non-overlapping laser spots. Intensities in various spots were optimized to reduce an objective function (5). With such chosen realistic spot size and positioning scheme we managed to reduce an objective function by a factor of 10. In Fig. 7 we plot in shades the required change in the high index dielectric in each of the focusing points. As expected, the largest change in the dielectric profile happens in the region of the largest geometric variation. As a rule, for slow weak variations we find that the absolute change α in the dielectric profile needed to compensate for the geometric variation, and an absolute strength of such a geometric variation δ are proportional to each other $\alpha \sim \delta$, which is consistent with predictions of perturbation theory.

6. STATISTICAL MODEL OF GEOMETRICAL IMPERFECTIONS FROM THE IMAGES OF 2D PHOTONIC CRYSTALS.

Manufacturing imperfections and tight tolerances in photonic crystals (PC) structures present great challenge on the road of transferring this revolutionary technology into the domain of commercial applications. Much work has been done to study an impact of imperfections on the performance of PCs. It was established quite generally that small degree of randomness in PC geometry and/or material constants leads to an overall reduction of a band gap size as well as an increased back scattering and radiation loss, while stronger randomness can lead to an appearance of localized impurity states. In the majority of theoretical studies various simplified models of randomness are assumed. Such models are frequently motivated by simplicity of parametrization of a particular type of randomness, or by the limitations of a modelling software, rather than by the presence of such perturbations in the experimentally implemented structures. In 1D PC multilayers one typically considers disorder in the thickness and value of a dielectric constant of individual layers. In 2D planar PCs and microstructured fibers one typically considers random displacement of features from an underlying ideal lattice, disorder in a feature size (radius of a hole, for example), refractive index disorder, distortion of features (ellipticity), as well as roughness of walls which are modelled as protrusions of some average characteristic hight and width. In 3D PCs derived from lithographical techniques and opals one typically

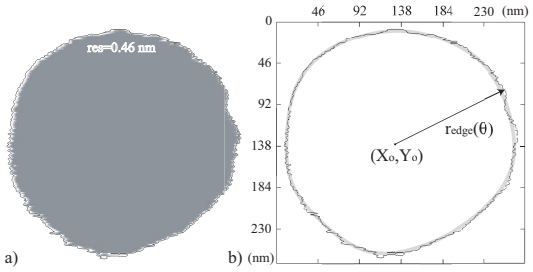

Figure 8. (a) Image of a hole together with a detected edge (b) Shape of a rugged edge is fitted with Fourier series in θ. Smooth curve is a fit with $N_m = 5$.

considers variation of layer thicknesses, variation in feature size, misalignment of individual features, stacking faults, and surface roughness. In these calculations disorder parameters are scanned from small to large and conclusions are drawn as to the effects of such a disorder. Propagation parameters can be sensitive functions of a disorder parameter. For example, intensity of back scattering from the wall roughness, and thus, propagation loss, in a planar TIR waveguide scales quadratically with roughness hight (from perturbation theory argument) and is a very sensitive function of a roughness correlation length. Thus, for a realistic comparison of theoretical estimates with experimental observations one has to be precise about statistical distribution of such a parameter. The goal of this section is to derive statistical properties of imperfections in 2D planar slab PCs from high resolution experimental images[33] to provide a realistic input to theoretical models.

6.1. Fitting shape of an individual feature

First, object recognition algorithm is used to extract circular features and their edges Fig. 8(a). We start with high resolution ($0.46nm$, $0.86nm$) images having few features. Edge of each hole is then fitted to extract coordinates of its center, radius, ellipticity and the higher order Fourier components in the edge shape Fig. 8(b). Particularly, we define an edge objective function

$$Q_{edge} = \frac{1}{N_{edge}} \sum_{i=1}^{N_{edge}} (r_{fit}(\theta_i) - r_{edge}(\theta_i))^2, \quad (6)$$

where $r_{edge}(\theta_i)$ is a distance from a hole center (X_0, Y_0) to an edge point (X_i, Y_i), and

$$r_{fit}(\theta_i) = R_0 + \sum_{m=2}^{N_m} (A_m Sin(\theta_i) + B_m Cos(\theta_i)). \quad (7)$$

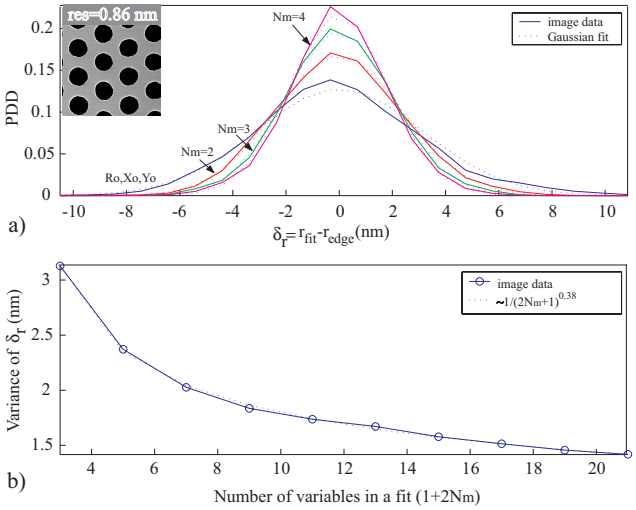

Figure 9. (a)Probability density distribution of a mismatch of a hole edge from a fitted smooth curve for a different number of angular momenta N_m in a fit. (b) Variance of a fit slowly decreases $\sim (1+2N)_m^{-0.38}$ as the number of angular momenta in a fit increases, suggesting that imperfections in circular features of 2D photonic crystals can not be characterized solely in terms of ellipticity.

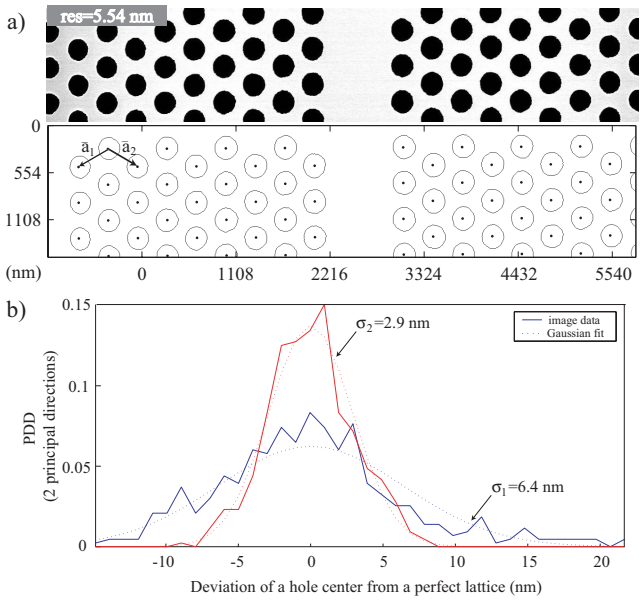

Figure 10. (a)2D photonic crystal lattice of holes with 2 missing rows (a waveguide) is analyzed. Edges of the holes are detected and a perfectly periodic underlying lattice is fitted to have its vertices (dots) closely matched with the hole centers (not shown). (b)2D PDD of the hole center deviations from the vertices of a perfect lattice. PDDs along 2 principal directions are shown: perpendicular to the waveguide σ_1, and parallel to the waveguide σ_2. Data distributions (solid lines) are fitted well with Gaussian profiles (dotted lines). Hole center deviations from an underlying lattice are highly anisotropic apparently because of the presence of a waveguide.

Note that $m = 0$ term in (7) corresponds to the hole radius, $m = 1$ terms are accounted by the hole center coordinates (X_0, Y_0), while $m = 2$ expansion coefficients define hole ellipticity. For a given N_m there are $(1 + 2N_m)$ fit parameters. We fit these parameters by minimizing an objective function (finding zeros of its derivatives) using multidimensional Newton method, where $\sqrt{Q_{edge}}$ characterizes the data variance around the fit.

6.2. Distribution of parameters defining a feature shape

If several holes are present the data is averaged over all features.

In Fig. 9(a) we present probability density distribution (PDD) of a random variable $\delta_r = (r_{fit}(\theta_i) - r_{edge}(\theta_i))$ when different numbers of angular momenta components N_m are included in the fit. We observe that image data (solid curves) and fitted Gaussian distribution (dotted curves) match well indicating that error of a fit is indeed Gaussian distributed. As the number of variables in a fit increases variance of δ_r becomes smaller Fig.9(b). We observe a slow power law decay of variance with the number of angular momenta components (from which fractal dimension of the roughness can be inferred), suggesting that imperfections in circular features can not be characterized solely in terms of ellipticity (which is frequently assumed in simulations), and that higher order angular components contribute considerably. High resolution image analyzed in Fig. 9 contained 11 holes. Averaged over the features we find that $R_0 = 124.3 \pm 1.8nm$, while ellipticity amplitude (7) $\sqrt{A_2^2 + B_2^2} = 2.7 \pm 1.2nm$ was found to be almost the same for any $N_m > 2$ used in the fit.

6.3. Displacement of features from their lattice positions

Next, lower resolution ($5.54nm$) images containing a large number of features (437 holes) were analyzed to determine distribution of deviations of the hole centers from an underlying perfect lattice Fig. 10(a). At first, coordinates of the hole centers $\bar{r}_0^i = (X_0^i, Y_0^i)$ were found by minimizing objective function (7) for various N_m. It was later found that statistics of deviations of the hole centers from an underlying perfect lattice is not sensitive to a particular choice of N_m. Parameters of an underlying perfect lattice were found by minimizing

a lattice objective function

$$Q_{lat} = \frac{1}{N_{holes}} \sum_{i}^{N_{holes}} (\bar{r}_0^i - n_1^i \bar{a}_1 - n_2^i \bar{a}_2)^2, \qquad (8)$$

where $\bar{a}_{1,2}$ are the basis vectors of an underlying perfect lattice, and $n_{1,2}^i$ are the integer lattice coordinates of a hole center i. It is relatively straightforward to find $2N_{holes}$ integer coordinates in (8) leaving 4 real parameters to fit. As before, we performed a fit with multi-dimensional Newton method. In Fig. 10(a) we present the edges of the holes together with the vertices of an underlying perfect lattice (dots). We now define a 2D random variable $\bar{\delta}_c = \bar{r}_0^i - n_1^i \bar{a}_1 - n_2^i \bar{a}_2$ which we assume to be 2D Gaussian distributed with PDD

$$\rho = \frac{1}{2\pi\sigma_1\sigma_2} exp(-\begin{pmatrix} \delta_c^x \\ \delta_c^y \end{pmatrix}^T R^T \begin{pmatrix} \frac{1}{2\sigma_1^2} & 0 \\ 0 & \frac{1}{2\sigma_2^2} \end{pmatrix} R \begin{pmatrix} \delta_c^x \\ \delta_c^y \end{pmatrix}), \qquad (9)$$

where $R = \begin{pmatrix} cos(\theta) & sin(\theta) \\ -sin(\theta) & cos(\theta) \end{pmatrix}$ is a 2D rotation matrix, and $\sigma_{1,2}$ are the variances along the two principle directions. Using the averages for a 2D Gaussian random variable, $< \delta_c^x \delta_c^x >= \sigma_1^2 cos^2(\theta) + \sigma_2^2 sin^2(\theta)$, $< \delta_c^y \delta_c^y >= \sigma_1^2 sin^2(\theta) + \sigma_2^2 cos^2(\theta)$, $< \delta_c^x \delta_c^y >= 2cos(\theta)sin(\theta)(\sigma_1^2 - \sigma_2^2)$ we deduce the distribution parameters $\sigma_{1,2}, \theta$. In Fig. 10(b) we plot PDD of $\bar{\delta}_c$ along the two principle directions ($\theta = -1.6^o$) from the lattice fit (solid lines) and a corresponding Gaussian distribution (dotted lines). We find that a 2D distribution of feature center displacements from the vertices of an underlying perfect lattice indeed appears to be Gaussian and is highly anisotropic as a symmetry breaking feature (waveguide) is present. The variance of the hole center deviations from a perfect lattice is twice as large $\sigma_1 = 6.4nm$ in the direction perpendicular to the waveguide than in the parallel direction $\sigma_2 = 2.9nm$.

7. CONCLUSION

In this work, we presented a general form of the coupled mode and perturbation theories to treat geometric variations of generic waveguide profiles with an arbitrary dielectric index contrast. Applications to various aspects of light propagation in deformed 2D photonic crystal waveguides were demonstrated. We conclude that semi-analytical CMT and PT can offer substantial computational advantages over time domain and frequency domain methods when analyzing the impacts of small imperfections or weak variations over large propagation distances. Together with input from statistical analysis of experimental images of planar 2D photonic crystals we believe that we now have a robust computational method and realistic model of roughness to make a direct comparison between simulations and measurements.

REFERENCES

1. Steven G. Johnson, Mihai Ibanescu, M. Skorobogatiy, Ori Weisberg, Torkel D. Engeness, Marin Soljačić, Steven A. Jacobs, J. D. Joannopoulos, and Yoel Fink, "Low-loss asymptotically single-mode propagation in large-core OmniGuide fibers," Opt. Express **9**, 748 (2001), http://www.opticsexpress.org/abstract.cfm?URI=OPEX-9-13-748.
2. Steven G. Johnson, Mihai Ibanescu, M. Skorobogatiy, Ori Weisberg, J. D. Joannopoulos, and Yoel Fink, "Perturbation theory for Maxwell's equations with shifting material boundaries," Phys. Rev. E **65**, 66611 (2002).
3. M. Skorobogatiy, Mihai Ibanescu, Steven G. Johnson, Ori Weisberg, Torkel D. Engeness, Marin Soljačić, Steven A. Jacobs, and Yoel Fink, "Analysis of general geometric scaling perturbations in a transmitting waveguide: fundamental connection between polarization-mode dispersion and group-velocity dispersion," J. Opt. Soc. Am. B **19**, (2002).
4. M. Skorobogatiy, Steven A. Jacobs, Steven G. Johnson, and Yoel Fink, "Dielectric profile variations in high index-contrast waveguides, coupled mode theory and perturbation expansions," Phys. Rev. E **67** ,46613 (2003).
5. M. Lohmeyer, N. Bahlmann, and P. Hertel, "Geometry tolerance estimation for rectangular dielectric waveguide devices by means of perturbation theory," Opt. Communications **163**, pp. 86–94 (1999).
6. N. R. Hill,"Integral-equation perturbative approach to optical scattering from rough surfaces," Phys. Rev. B **24**, p. 7112 (1981).
7. D. Marcuse, *Theory of dielectric optical waveguides* (Academic Press, 2nd ed., 1991).
8. A. W. Snyder and J. D. Love, *Optical waveguide theory* (Chapman and Hall, London, 1983).
9. B. Z. Katsenelenbaum, L. Mercader del Río, M. Pereyaslavets, M. Sorolla Ayza, and M. Thumm, *Theory of Nonuniform Waveguides: The Cross-Section Method* (Inst. of Electrical Engineers, London, 1998).
10. L. Lewin, D. C. Chang, and E. F. Kuester, *Electromagnetic waves and curved structures* (IEE Press, Peter Peregrinus Ltd., Stevenage 1977).

11. F. Sporleder and H. G. Unger, *Waveguide tapers transitions and couplers* (IEE Press, Peter Peregrinus Ltd., Stevenage 1979).
12. H. Hung-Chia, *Coupled mode theory as applied to microwave and optical transmission* (VNU Science Press, Utrecht 1984).
13. Steven G. Johnson, P. Bienstman, M. A. Skorobogatiy, M. Ibanescu, E. Lidorikis, and J. D. Joannopoulos "The adiabatic theorem and a continuous coupled-mode theory for efficient taper transitions in photonic crystals," Phys. Rev. E **66**,66608 (2002).
14. N.A. Mortensen, M.D. Nielsen, J.R. Folkenberg, K.P. Hansen, and J. Laegsgaard, "Small-core photonic crystal fibers with weakly disordered air-hole claddings," J. Opt. A, **6**, 221 (2004).
15. A.A. Asatryan, P.A. Robinson, L.C. Botten, R.C. McPhedran, N.A. Nicorovici, and C. Martijn de Sterke, "Effects of disorder on wave propagation in two-dimensional ptotonic crystals," Phys. Rev. E **60**,6118 (1999).
16. A.A. Asatryan, P.A. Robinson, L.C. Botten, R.C. McPhedran, N.A. Nicorovici, and C. Martijn de Sterke, "Effects of geometric and refractive index disorder on wave propagation in two-dimensional ptotonic crystals," Phys. Rev. E **62**,5711 (2000).
17. T.N. Langtry, A.A. Asatryan, L.C. Botten, C. Martijn de Sterke, R.C. McPhedran, and P.A. Robinson, "Effects of disorder in two-dimensional ptotonic crystal waveguides," Phys. Rev. E **68**,26611 (2003).
18. B.C. Gupta, and Z. Ye, "Disorder effects on the imaging of a negative refractive lens made by arrays of dielectric cylinders," J. Appl. Phys **94**, 2173 (2003).
19. A.G. Martin, D. Hermann, F. Hagmann, K. Busch, and P. Wolfle, "Defect computations in photonic crystals: a solid state theoretical approach," Nanotechnology **14**, 177 (2003).
20. S. Lan, K. Kanamoto, T. Yang, S. Nishikawa, Y. Sugimoto, N. Ikeda, H. Nakamura, K. Asakawa, and H. Ishikawa, "Similar role of waveguide bends in photonic crystal circuits and disordered defects in coupled cavity waveguides: An intrinsic problem in realizing photonic crystal circuits," Phys. Rev. B **67**, 115208 (2003).
21. S. Fan, P.R. Villeneuve, and J.D. Joannopoulos, "Theoretical investigation of fabrication-related disorder on the properties of photonic crystals," J. Appl. Phys. **78**, 1415 (1995).
22. W. Zhi, R. Guobin, and L. Shuqin, "Mode disorder in elliptical hole PCF,"Optical Fiber Tech. **10**, 124 (2004).
23. M.A. Kaliteevski, J.M. Martinez, D. Cassagne, and J.P. Albert, "Disorder-induced modification of the transmission of light in a two-dimensional photonic crystal," Phys. Rev. B **66**, 113101 (2002).
24. W. Bogaerts, P. Bienstman, and R. Baets, "Scattering at sidewall roughness in photonic crystal slabs," Opt. Lett. **28**, 689 (2003).
25. M.L. Povinelli, S.G. Johnson, E. Lidorikis, J.D. Joannopoulos, M. Soljacic, "Effect of a photonic band gap on scattering from waveguide disorder," Appl. Phys. Lett. **84**, 3639 (2004)
26. R. Holland, "Finite-difference solution of Maxell's equation in generalized nonorhogonal coordinates," IEEE Trans. Nucl. Sci. **30**, 4589 (1983).
27. J.P. Plumey, G. Granet, and J. Chandezon, "Differential covariant formalism for solving Maxwell's equations in curvilinear coordinates: oblique scattering from lossy periodic surfaces," IEEE Trans. on Antennas Propag. **43**, 835 (1995).
28. E.J. Post, *Formal Structure of Electromagnetics* (Amsterdam: North-Holland, 1962).
29. F.L. Teixeira and W.C. Chew, "Analytical derivation of a conformal perfectly matched absorber for electromagnetic waves," Microwave Opt. Technol. Lett. **17**, 231 (1998).
30. M. Skorobogatiy, Steven A. Jacobs, Steven G. Johnson, and Yoel Fink, "Geometric variations in high index-contrast waveguides, coupled mode theory in curvilinear coordinates," Opt. Express **10**, 1227 (2002), http://www.opticsexpress.org/abstract.cfm?URI=OPEX-10-21-1227.
31. M. Skorobogatiy, "Modeling the impact of imperfections in high-index-contrast photonic waveguides ," Phys. Rev. E **70**, 46609 (2004).
32. P. Bienstman, software at http://camfr.sf.net.
33. Experimental images used in this paper are courtesy of Prof. Ann Talneau, CNRS, Lab Photon & Nanostruct, Route Nozay, Marcoussis, F-91460 France.